Supporting Information

Polylactic acid/chitosan-IKVAV Janus film serving as a dual functional platform for spinal cord injury repair

Liyang Yu,[a‡] Haoyong Jin,[b,c‡] He Xia,[a‡] Xiaoxiong Wang,[d] Liang Wang,[a] Dezheng Li,[a] Jiangli Zhao,[b,c] Yuanhua Sang,[a] Jichuan Qiu,[a] Ning Lu,[e] Hong Liu[a*] and Ning Yang[b,c*]*

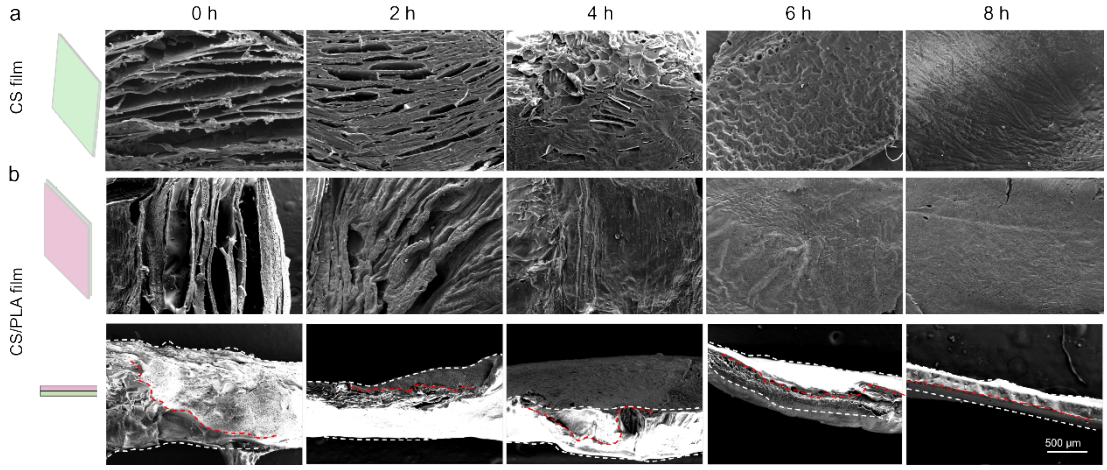

Figure S1. Electron Probe X-ray Micro-Analyzer (EPMA) images of the surface of CS films after drying for 0, 2, 4, 6, and 8 h, respectively, followed by freeze-dying. b) EPMA images of the PLA surface and the lateral side of the PLA/CS Janus films prepared on different CS films in (a). The dashed red line indicates the interface between PLA and CS. The top side is PLA.

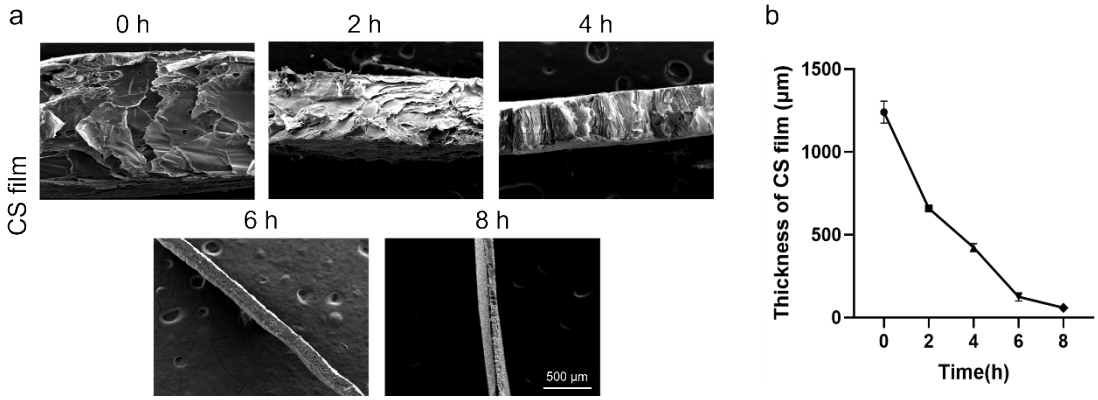

Figure S2. a) EPMA images of the lateral side of CS film after drying for 0, 2, 4, 6, and 8 h, respectively, followed by freeze-dying. b) Thickness variation of CS film at different drying times.

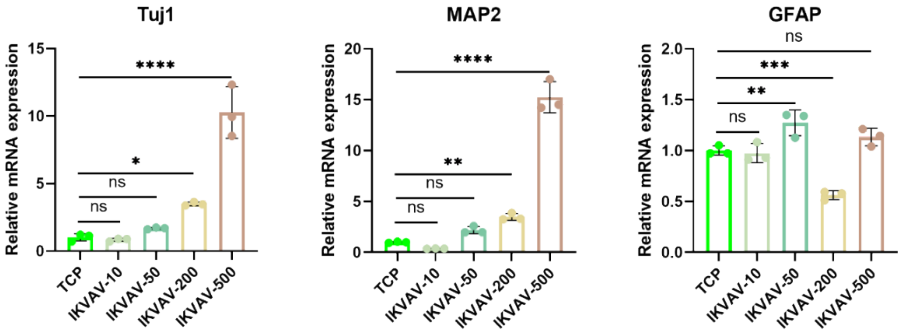

Figure S3. RT-qPCR results of the neural-specific genes including Tuj1, MAP2, and GFAP of NSCs cultured with IKVAV peptides at concentrations of 10 (IKVAV-10), 50 (IKVAV-50), 200 (IKVAV-200), 500 (IKVAV-500) μM at day 5. n = 3, *p < 0.05, **p < 0.01, ***p < 0.001, and ****p < 0.0001.

We investigated the influence of IKVAV peptide concentration on the differentiation of NSCs. After the NSCs were incubated with IKVAV for 5 days, the mRNA expression of neural specific markers including beta tubulin III (Tuj1), microtubule-associated protein 2 (MAP2), and glial fibrillary protein (GFAP) were analyzed by real-time quantitative polymerase chain reaction (RT-qPCR). When the IKVAV concentration was 500 μM, the mRNA expression of Tuj1 and MAP2 was highest among all groups, suggesting that 500 μM of IKVAV could significantly promote the neuronal differentiation of NSCs. To this end, we used 500 μM of IKVAV in the following experiment.

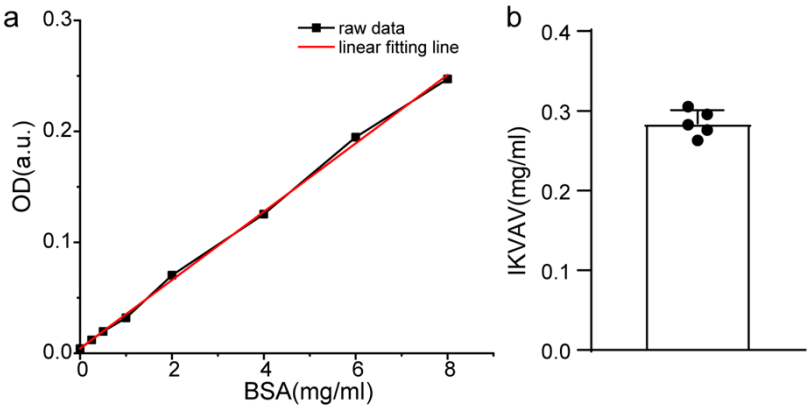

Figure S4. a) Standard Curve for Biuret method of protein detection kit. b) Detection concentration of IKVAV on CS-IKVAV film. n = 5.

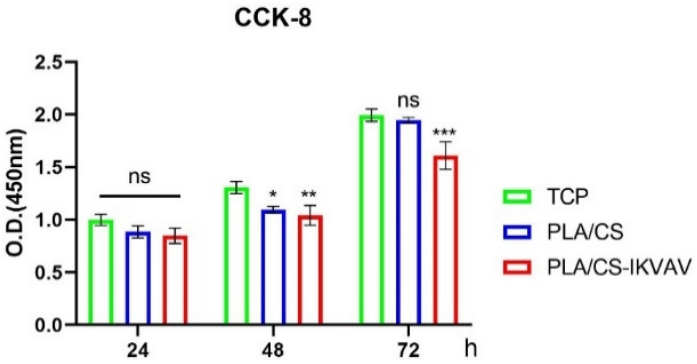

Figure S5. CCK-8 assay of NSCs seeding on TCP and chitosan side of the PLA/CS and PLA/CS-IKVAV Janus films at 24, 48, and 72 h. n = 5, *p < 0.05, **p < 0.01, and ***p < 0.001.

The viability of NSCs in all groups gradually increased from 24 to 72 h. At 24 hours, the viability of the NSCs was similar in all groups. However, at 72 hours, the cell viability of the PLA/CS-IKVAV group was lower than that of TCP, which might be due to accelerated differentiation of NSCs.

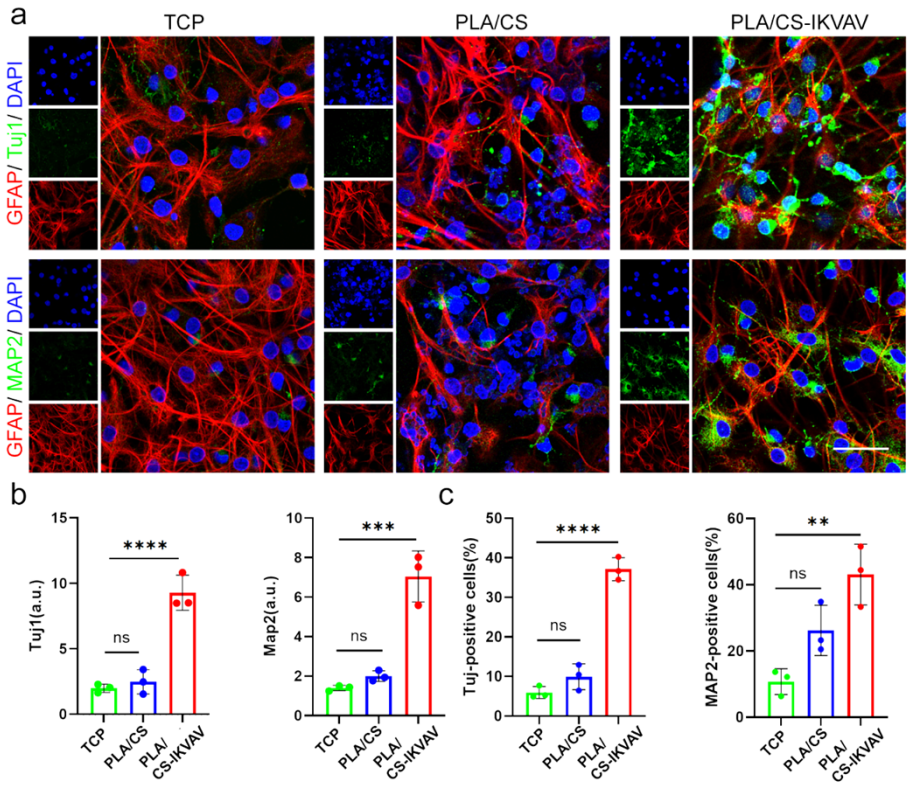

Figure S6. a) Immunofluorescence staining of the neural-specific markers, including Tuj1, MAP2, and GFAP after NSCs were seeded on TCP, PLA/CS, and PLA/CS-IKVAV Janus films for 7 days. The Tuj1, MAP2, and nuclei were stained into green, red, and blue, respectively. Scale bar, 25 μm. b) Average fluorescence intensity of Tuj1 and MAP2 of TCP, PLA/CS, and PLA/CS-IKVAV Janus groups obtained based on images in (a). c) Percentages of Tuj1- or MAP2-positive cells in TCP, PLA/CS, and PLA/CS-IKVAV groups obtained based on images in (a). n = 3, **p < 0.01, ***p < 0.001, and ****p < 0.0001.

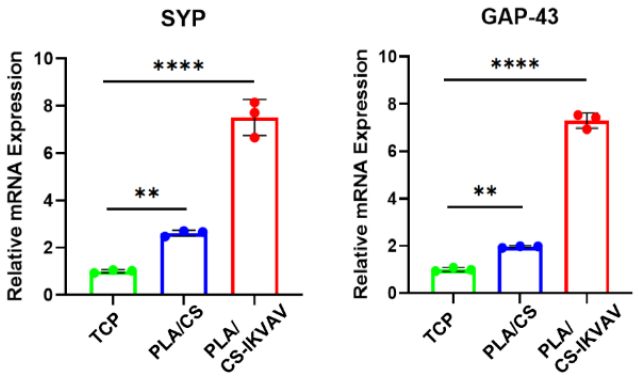

Figure S7. RT-qPCR analysis of the synapse-associated genes after NSCs were seeded on TCP, PLA/CS, and PLA/CS-IKVAV substrates for 7 days. n = 3, **p < 0.01, ***p < 0.001, and ****p < 0.0001.

In addition, we examined the mRNA levels of SYP and GAP-43 at the gene level by RT-qPCR for each group 7 days after seeding (Fig. S6b, Supporting Information). The mRNA levels of SYP were ≈2.61 and ≈7.51-fold higher in PLA/CS and PLA/CS-IKVAV than in TCP group, respectively. And mRNA levels of GAP-43 increased 1.97-fold (PLA/CS) and 7.30-fold (PLA/CS-IKVAV), respectively.

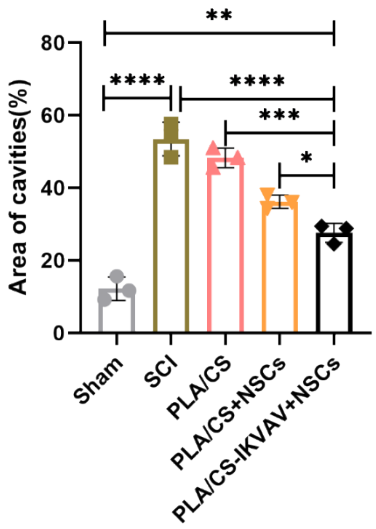

Figure S8. Statistical analysis of the average cavities of the spinal cord tissue of the rats in the Sham, SCI, PLA/CS, PLA/CS+NSCs, and PLA/CS-IKVAV+NSCs groups at week 6 post-surgery. n = 3, *p < 0.05, **p < 0.01, and ****p < 0.0001.

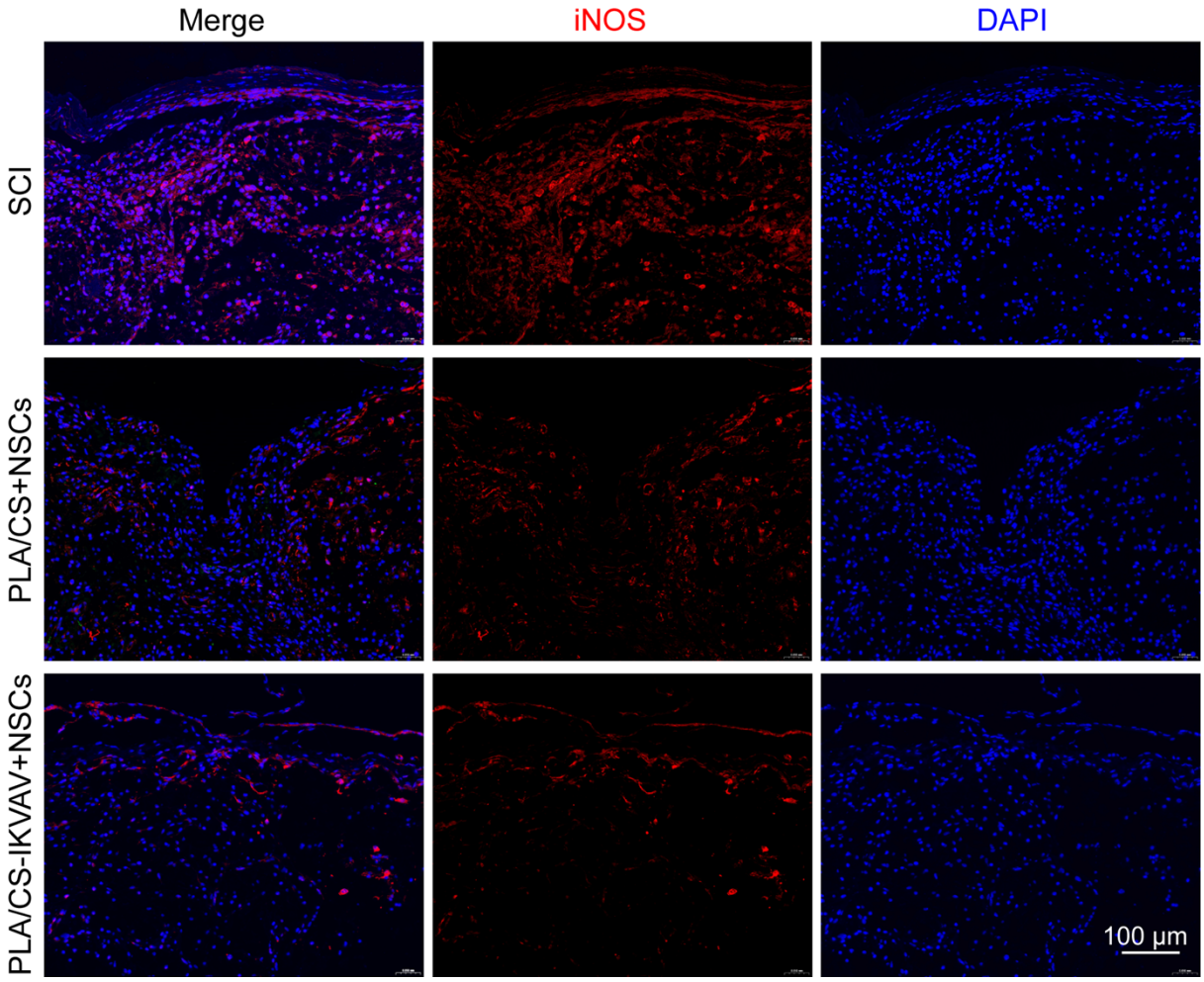

Figure S9. Immunofluorescence staining images of iNOS in PLA/CS+NSCs and PLA/CS-IKVAV+NSCs groups at day 7 after SCI. The iNOS and nuclei were stained into red and blue, respectively.

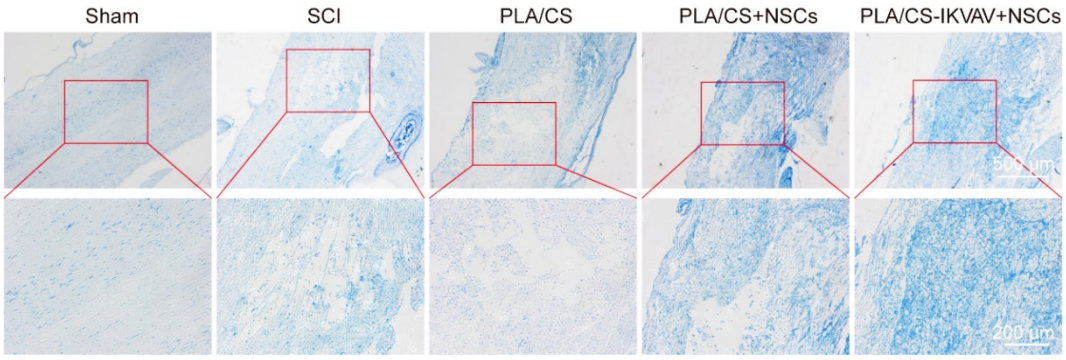

Figure S10. Nissl staining of spinal cord tissues of rats in the Sham, SCI, PLA/CS, PLA/CS+NSCs, and PLA/CS-IKVAV+NSCs group at week 6 post-surgery.

In the Sham group, the structure of neurons was intact and Nissl bodies were evenly distributed. Compared with the Sham group, the number of Nissl bodies in the SCI group was significantly reduced and the color was lighter, which showed severe neuronal damage. The volume of Nissl bodies in the PLA/CS group increased compared with that in the SCI group. The volume and number of Nissl bodies in the PLA/CS+NSCs group were both increased and the color was darker. In contrast, the PLA/CS-IKVAV+NSCs group displayed a more complete organizational structure with more neurons and Nissl bodies.

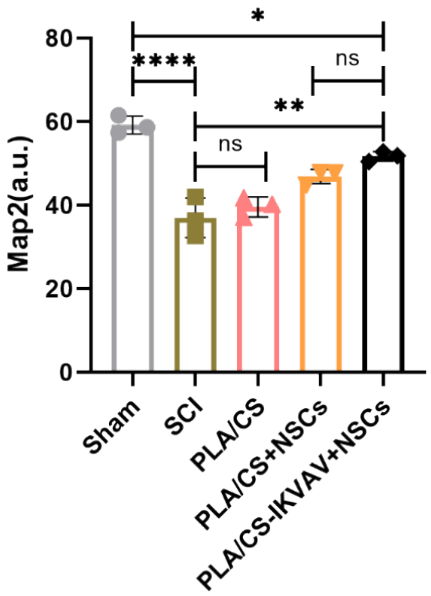

Figure S11. The average fluorescence intensity of MAP2 in the TCP, PLA/CS, PLA/CS+NSCs, and PLA/CS-IKVAV+NSCs groups was obtained based on Figure 6b. n = 3, *p < 0.05, **p < 0.01, ***p < 0.001, and ****p < 0.0001.

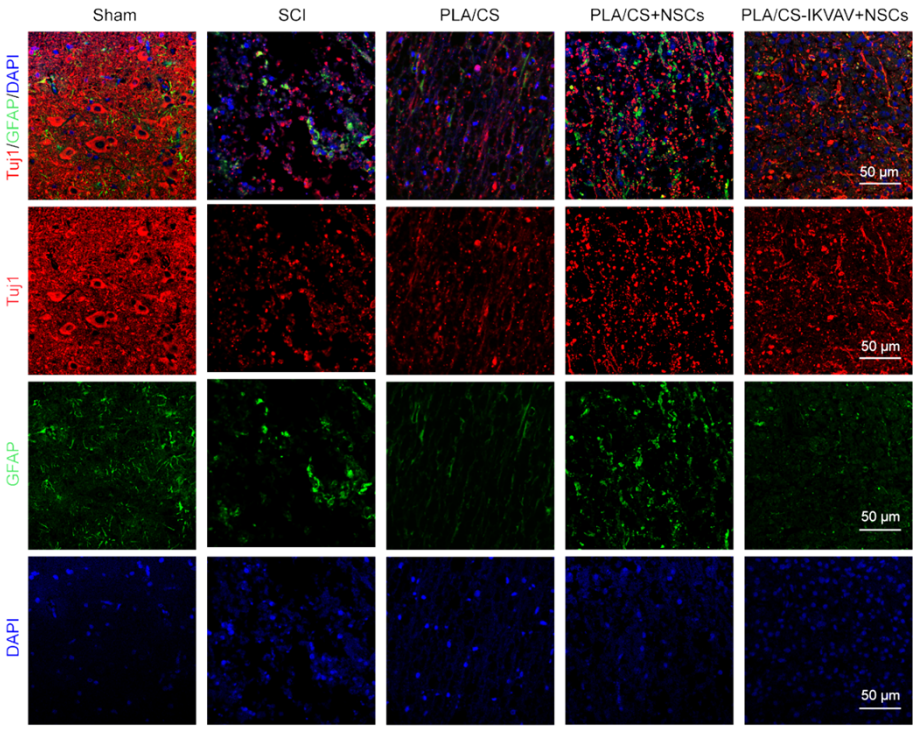

Figure S12. Immunofluorescence staining results of the spinal cord tissue of rats in the Sham, SCI, PLA/CS, PLA/CS+NSCs, and PLA/CS-IKVAV+NSCs groups at week 6. The MAP2, GFAP, and nuclei were stained into red, green, and blue, respectively.

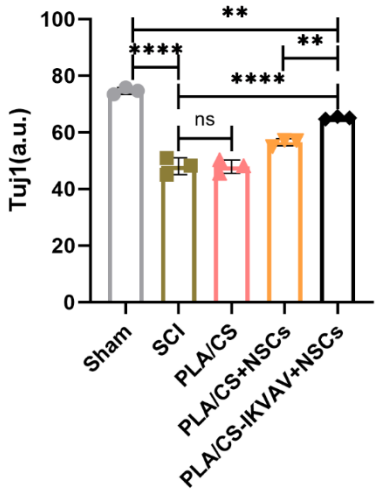

Figure S13. Average fluorescence intensity of Tuj1 in the TCP, PLA/CS, PLA/CA+NSCs, and PLA/CS-IKVAV+NSCs group. n = 3, *p < 0.05, **p < 0.01, ***p < 0.001, and ****p < 0.0001.

The mean fluorescence intensity of Tuj1 was quantified from three randomly selected images, normalized to the SCI group. There was no difference between PLA/CS and SCI

groups. The mean fluorescence intensity in the PLA/CS+NSCs group and the PLA/CS-IKVAV+NSCs group was ≈1.27 and 1.38 times higher than that in the SCI group, respectively.

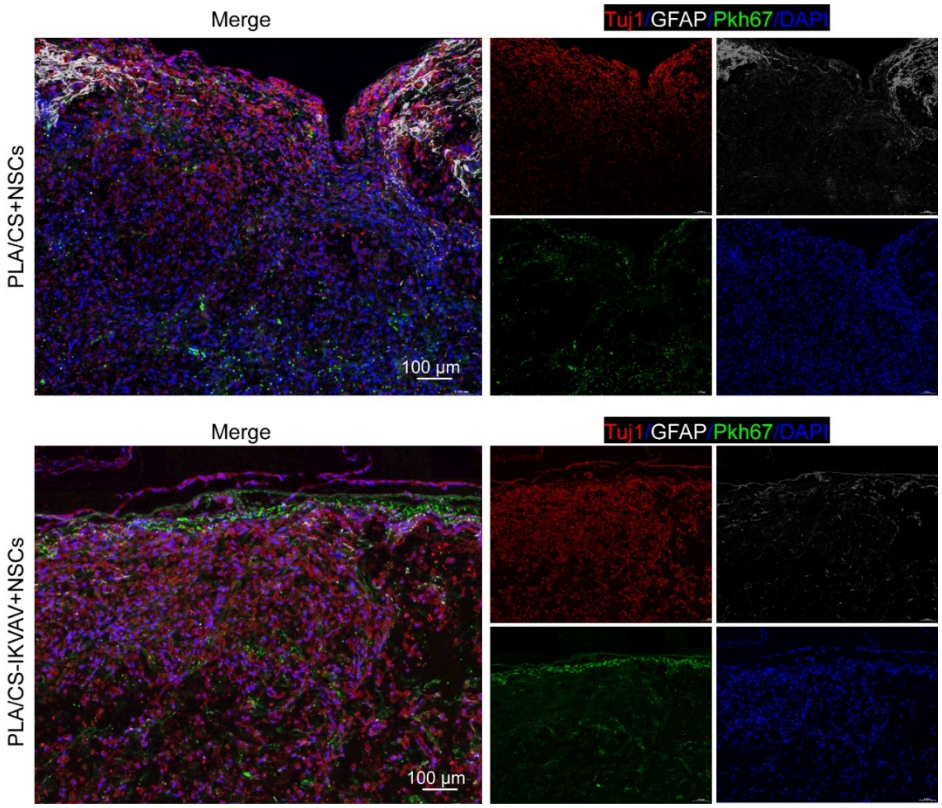

Figure S14. Immunofluorescence staining images of the spinal cord tissue of rats in PLA/CS+NSCs and PLA/CS-IKVAV+NSCs groups at day 7. Pkh67-labeled NSCs were shown in green, while Tuj1, GFAP, and nuclei were stained into red, white, and blue, respectively.

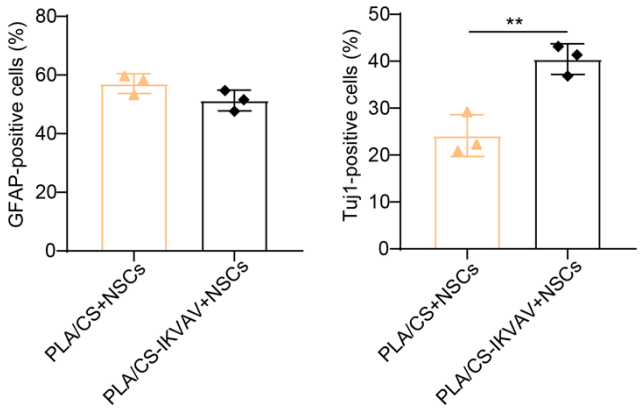

Figure S15. Statistical analysis of the percentages of GFAP- or Tuj1- positive cells in PLA/CS and PLA/CS-IKVAV groups was obtained based on Figure S14. n=3, **p < 0.01.

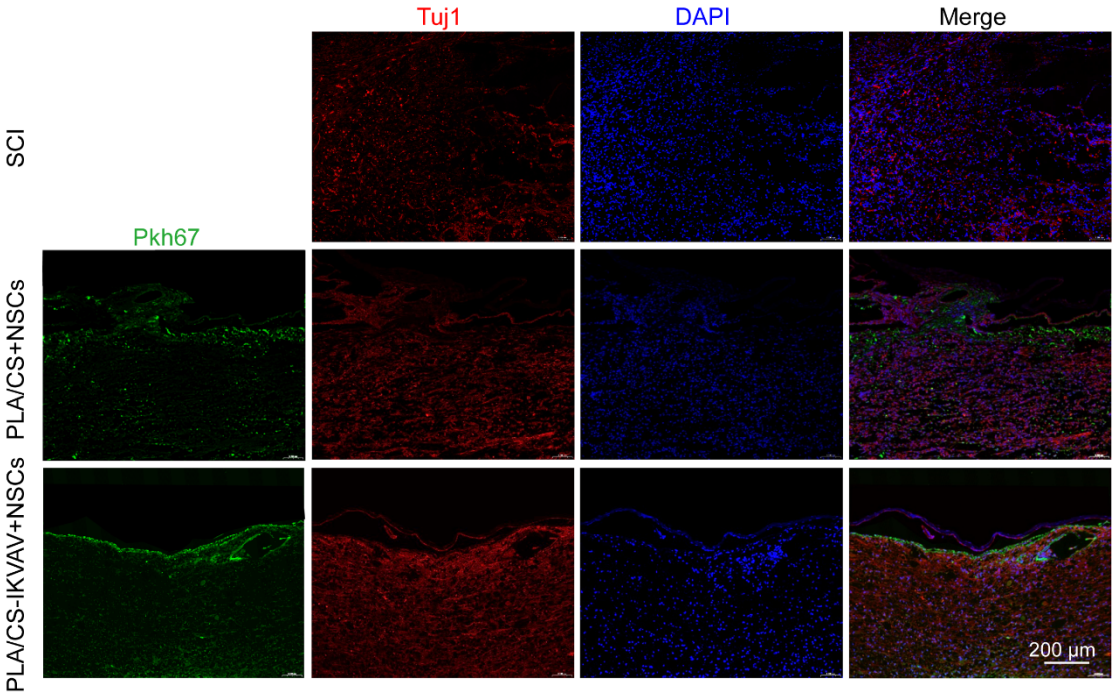

Figure S16. Immunofluorescence images of the spinal cord tissues of the rats in SCI, PLA/CS+NSCs, and PLA/CS-IKVAV+NSCs groups at day 14. Pkh67-labeled NSCs were shown in green, while Tuj1 and nuclei were stained into red and blue, respectively.

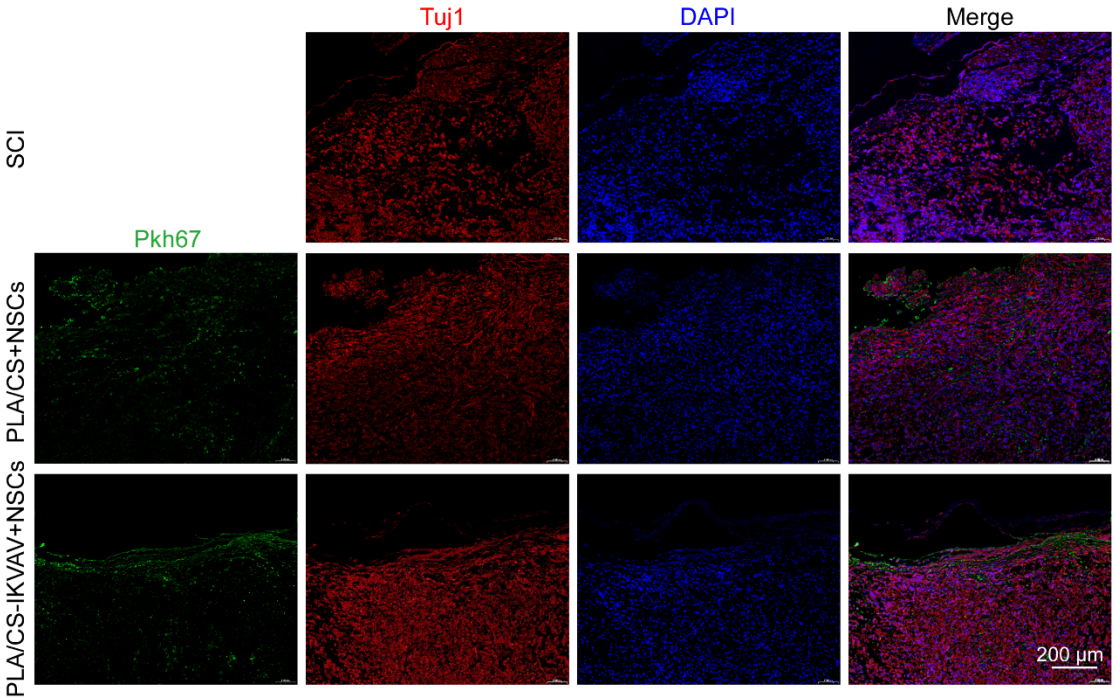

Figure S17. Immunofluorescence images of the spinal cord tissues of the rats in SCI,

PLA/CS+NSCs, and PLA/CS-IKVAV+NSCs groups at day 28. Pkh67-labeled NSCs were shown in green, while Tuj1 and nuclei were stained into red and blue, respectively.

Table S1. Sequences of RT-qPCR primers.

Gene	Forward primers (5‘-3‘)	Reverse primers (5‘-3‘)
Actin	CTCTGTGTGGATTGGTGGCT	CGCAGCTCAGTAACAGTCCG
Tuj1	CAACTATGTGGGGGACTCGG	TGGCTCTGGGCACATACTTG
MAP2	CCAACACTAGCGGAACGATG	ACTTGGGTAGTTTGCCCTCC
GFAP	TTGACCTGCGACCTTGAGTC	GAGTGCCTCCTGGTAACTCG
SYP	TGCCATCTTCGCCTTTGCTA	CTCTCCGTCTTGTTGGCACA
GAP43	AGATGGTGTCAAACCGGAGG	TCTCCACACCATCAGCAACG

Table S2. Relevant antibodies

Target protein	Catalogue No	Application	Manufacturer
Tuj1 (M)	ab78078	IF (1:1000); WB (1:5000)	Abcam,USA
MAP2 (M)	ab11267	IF (1:600); WB (1:5000)	Abcam,USA
GFAP (R)	16825-1-AP	IF (1:1500); WB (1:5000)	Proteintech, USA
SYP (R)	17785-1-AP	IF (1:800)	Proteintech, USA
GAP43 (R)	ab75810	IF (1:400)	Abcam, USA
GAPDH (R)	10494-1-AP	WB (1:5000)	Proteintech, USA
iNOS (R)	ab178945	IF (1:500)	Abcam, USA
Goat Anti-Rabbit IgG H&L (Alexa Fluor® 594)	ab150080	IF (1:1000)	Abcam, USA

Goat Anti-Mouse IgG H&L (Alexa Fluor® 488)	ab150113	IF (1:1000)	Abcam, USA
Goat Anti-Rabbit IgG H&L (Alexa Fluor® 488)	ab150077	IF (1:1000)	Abcam, USA
Goat Anti-Mouse IgG H&L (Alexa Fluor® 594)	ab150116	IF (1:1000)	Abcam, USA

Annotation: M: Mouse antibody; R: Rabbit antibody; IF: Immunofluorescent stain; WB: Western blotting